



Evaluation of In-Die Compression Data for a Deeper Understanding of Altered Excipient Properties upon Temperature Rise

Hanna Dorothea Grumann¹ · Stefan Klinken¹ · Peter Kleinebudde¹

Received: 6 January 2023 / Accepted: 7 March 2023
© The Author(s) 2023

Abstract

The thermodynamic analysis of tablet formation includes the thermal and mechanical analysis during compression. The aim of this study was to evaluate alterations of force–displacement data upon temperature rise as an indicator for changed excipient properties. The tablet press was equipped with a thermally controlled die to imitate the heat evolution from tableting on an industrial scale. Six predominantly ductile polymers with a comparably low glass transition temperature were tableted at temperatures ranging from 22–70°C. Lactose served as a brittle reference with a high melting point. The energy analysis included the net and recovery work during compression, from which the plasticity factor was calculated. The respective results were compared to the changes in compressibility obtained via Heckel analysis. Elevated temperatures reduced the necessary work for plastic deformation for the ductile polymers, which was reflected in decreasing values for the net work of compaction and the plasticity factor. The recovery work slightly increased for the maximum tableting temperature. Lactose showed no response to temperature variations. Changes in the net work of compaction showed a linear correlation to the changes in yield pressure, which could be correlated to the glass transition temperature of a material. It is therefore possible to detect material alterations directly from the compression data, if the glass transition temperature of a material is sufficiently low.

Keywords deformation behavior · energy parameters · force–displacement · heated tableting · plasticity factor

Introduction

Direct compression is a commonly known technique for the manufacture of tablets. The mechanical strength of a compact is dependent on the bonding strength from molecular interactions and the established bonding area [1, 2]. During a compression cycle, powder consolidation includes rearrangement, slippage, and elastic and plastic deformation as well as fragmentation [1]. Sufficient tablet integrity therefore requires energy input, which is partially lost to heat generation [3–5]. A significant temperature rise during tableting has been proven in several studies [5–9]. Local temperatures > 100°C have been discussed [10]. This might affect the resulting tablet characteristics if the physicochemical properties of a material are thereby altered [11].

For the thermodynamic analysis of tablet formation, the consumed work and generated heat during compression have been subject to numerous studies. The thermal analysis includes infrared thermography [6–8], calorimetry [9, 12–15], and finite element analysis [5, 16]. Changes in temperature arise from the conversion of mechanical to thermal energy. The mechanical energy input can be derived from force–displacement profiles, which provide detailed information about a powder's compression behavior [17–19]. Their shape is influenced by the material properties, the tableting equipment, and the applied settings [20]. From the calculated distance between the punches, the compact height and porosity during compression can be evaluated simultaneously [21]. Several widely used compression equations relate the porosity, or the respective relative density, to the applied pressure [22, 23]. These methods, including Heckel analysis, can be utilized to characterize the mechanistic deformation behavior of materials. Although the temperature might rise drastically during prolonged compression periods, the influence of the generated heat on energy parameters has rarely been studied. To serve this purpose, either the production process needs to be run for a significant time or the

✉ Peter Kleinebudde
kleinebudde@hhu.de

¹ Institute of Pharmaceutics and Biopharmaceutics, Heinrich Heine University, Universitätsstraße 1, 40225 Duesseldorf, Germany



powder has to be heated before compression to mimic the temperature rise on an industrial scale. Ketolainen *et al.* [6] correlated the mechanical and thermal energy when a tableting process was run for a maximum of 65 min. The investigation included microcrystalline cellulose (MCC) and dicalcium phosphate dihydrate (DCPDH), which were tableted with and without lubrication. While a drastic temperature change could be observed for some formulations, the energy parameters remained unchanged after an initial stabilization period. It is unlikely, however, that MCC and DCPDH were thermally affected by the evolving heat. For MCC, three step transitions upon heating have been identified at 132, 159, and 184°C via differential scanning calorimetry [24], while DCPDH also shows no event until it dehydrates above 100°C [25]. Those temperatures were clearly not reached during the tableting procedure. Cespi *et al.* [26] analyzed the temperature-dependent mechanical properties of four common pharmaceutical excipients using a fan heater within a modified tablet press. Heckel and energy analysis revealed a notable influence on the ductility of materials that undergo a thermally induced transition, while there was no considerable effect on the calculated energy values. It was concluded that either the effect was too weak or the investigation of energetic indexes is not sufficiently sensitive. The results were confirmed in a subsequent study investigating blends of acetylsalicylic acid and polyethylene oxides with different molecular weights [27]. In both studies, however, there was either no thermal transition in the investigated temperature range or it was only faint when the glass transition temperature (T_g) of a material was approached. In another study of Partheniadis *et al.* [11], the elevated temperatures were generated by a heating element, which was fitted to the die. A decrease in the work of compaction for a polymer with a T_g close to the tableting temperature was noted, which was explained with a decrease in friction as the material transforms to the viscous state.

Hence, it appears reasonable to consider a polymer's thermal sensitivity when evaluating energy parameters. In ductile materials, the T_g can be identified as a crucial parameter for compression experiments. Upon temperature rise, polymers leave the rigid state and become more deformable, as their molecular mobility increases [28]. This affects their compressibility, which is the capacity of a powder to reduce its volume upon pressure [29]. When the compressibility is evaluated using Heckel analysis, a temperature-dependent decrease in yield pressure (P_y) has frequently been observed, which is influenced by the T_g of a material [11, 26, 30, 31]. The reduced resistance against deformation promotes a higher strength of compacts after tableting [10]. As in-die Heckel analysis is derived from parts of the force–displacement data, changes in P_y should also be reflected in the energy calculation.

The aim of this study was to evaluate in-die compression data as a tool for changed excipient properties upon temperature rise and their correlation to the T_g of a material. In contrast to a previous study, the equilibration time of the powder within the die was kept short to mimic the temperature increase on an industrial scale [32]. The applicability of the plasticity factor, as introduced by Stamm and Mathis [33], was critically assessed for elevated temperatures. The T_g of all investigated polymers was within or closely above the investigated temperature range.

Materials and Methods

Materials

The investigated excipients are listed in Table I. Lactose was chosen as a mostly crystalline reference with a high melting point and brittle compaction properties. All used polymers have a comparably low T_g and show predominantly plastic behavior, which results from an amorphous or partially crystalline structure.

Methods

Particle Density

Particle densities were determined according to USP <699> using helium pycnometry (AccuPyc 1330, Micromeritics, USA) [36]. Measurements were performed at $25 \pm 0.1^\circ\text{C}$ ($n=3$).

Powder Compression

Tableting experiments were conducted on a STYL'One Evo compaction simulator (Medelpharm, France), which was equipped with a thermally controlled die. The detailed set-up has previously been described [32]. Tableting was performed maintaining a die temperature of 22, 30, 50, or 70°C, respectively, using flat-faced, round EuroD punches with a diameter of 11.28 mm. All materials were stored in a climate room (21°C, 45% r.h.) for at least 7 days before processing. After lubricating the die with a brush, it was filled gravimetrically due to the low bulk density of the excipients (tablet weight ~350 mg). Between the end of filling and the start of a tableting cycle, a time period of 2–3 s was exemplarily monitored. All excipients were compressed at 250 MPa maximum compression pressure with an acquisition frequency of 10 kHz ($n=3$). The tableting speed was set to 25% in force mode (1-compression), which corresponds to an average upper punch speed of 15 mm/s and lower punch speed of 39 mm/s.

Table 1 List of the Investigated Excipients

Trade name	Abbreviation	Chemical composition	Supplier	T/°C
Flowlac® 100	FL	α -Lactose monohydrate	Meggle (Germany)	216 ^{m*}
Kollidon® SR	KSR	Polyvinyl acetate, polyvinylpyrrolidone, sodium lauryl sulfate, and silica (ratio 8:1.9:0.08:0.02)	BASF (Germany)	42 ^{g*}
Eudragit® E PO	EPO	Copolymer of N,N-dimethylaminoethyl methacrylate, methyl methacrylate, and butyl methacrylate	Evonik Industries (Germany)	49 ^{g*}
Eudragit® RS PO	RS	Copolymer of ethyl acrylate, methyl methacrylate, and methacrylic acid ester	Evonik Industries (Germany)	58 ^{g*}
Eudragit® RL PO	RL	Copolymer of ethyl acrylate, methyl methacrylate, and methacrylic acid ester	Evonik Industries (Germany)	70 ^{g*}
Soluplus®	SP	Copolymer of polyvinyl caprolactam, polyvinyl acetate, and polyethylene glycol	BASF (Germany)	75 ^{g*}
Nisso HPC SSL	SSL	Hydroxypropyl cellulose	Nippon Soda (Japan)	82 ^{g**}
Parateck® LUB MST	-	Magnesium stearate	Merck (Germany)	140 ^{g***}

m, Melting; g, Glass Transition ^{*}[32], ^{**}[34], ^{***}[35]

Compression Analysis

Compressibility The compressibility of all materials was investigated using in-die Heckel analysis, where the negative natural logarithm of the in-die porosity (ϵ) of a tablet is plotted against the applied compression pressure. ϵ was calculated from the in-die solid fraction (SF):

$$\epsilon = 1 - SF \quad (1)$$

with

$$SF = \frac{\rho_t \left[\frac{mg}{mm^3} \right]}{\rho_p \left[\frac{mg}{mm^3} \right]} \quad (2)$$

SF contains the tablet density ρ_t and the particle density ρ_p , which was determined as described in the “[Particle Density](#)” section. The tablet density was obtained from the tablet weight w after ejection and the tablet volume V during compression:

$$\rho_t = \frac{w[mg]}{V[mm^3]} \quad (3)$$

The data pre-processing and evaluation was executed with an in-house written Python 3.9 program (EvTab 1.6.3.), where a threshold of 1 MPa for the upper punch indicated the starting point of the compression cycle. The mean yield pressure (P_y) was identified by linear regression of the linear region, which is located between the starting point and the maximum compression pressure of the respective tableting cycle. P_y can be obtained from the reciprocal slope of the regression line using Eq. 4:

$$-\ln(\epsilon) = \frac{1}{P_y} P + A \quad (4)$$

where P is the applied pressure in MPa and A is the y-axis intercept. The linear region was identified using a recursive, excluding algorithm, which was based on a coefficient of determination limit for the linear, least square regression via the stats.linregress algorithm of SciPy 1.7.2 of 0.988. All measurements were performed in triplicate.

Energy Analysis The mechanical energy input of a tablet machine can be derived from force–displacement measurements. The force–displacement analysis of both punches was calculated from the distance between the upper and the lower punch (x) at any time during the compression cycle using an in-house written Python 3.9 program (EvTab 1.6.3.). The acquisition frequency was set to 10 kHz. Typically, the gross energy input of one punch corresponds to the area under the trace ABC (AUC_{ABC} , Fig. 1). It contains the dissipated energy from friction (E_1) and the compressive work (E_{cw}). E_{cw} is the sum of the net work of compaction E_2 (AUC_{abD}) and the elastic work E_3 (AUC_{DBC}) [37]. Hence, the following relationships can be defined:

$$\begin{aligned} E_2 &= AUC_{abC} - AUC_{DBC} \\ E_2 &= E_{cw} - E_3 \end{aligned} \quad (5)$$

The energy E_2 was calculated using the trapezoid rule [18, 38]:

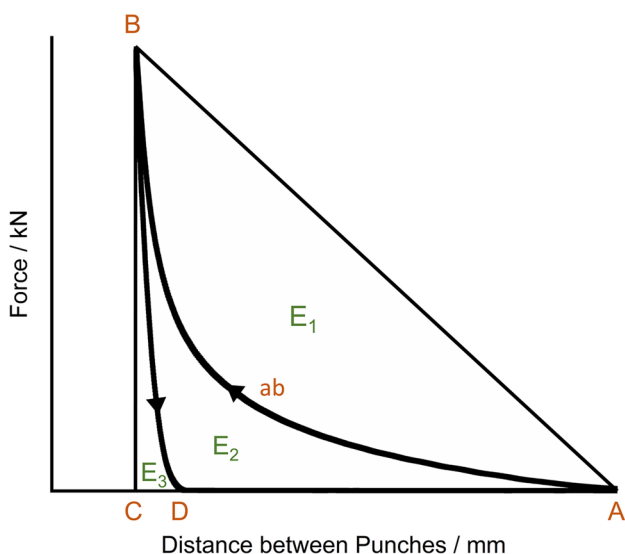


Fig. 1 Characteristic compression cycle with the associated energy parameters

$$E_2 = \int_{x_{max}}^{x_{min}} F(x) * dx - \int_{x_{min}}^{x_{od}} F(x) * dx \tag{6}$$

where x_{max} is the distance between punches at which the force F rises from 0 as a function of $F(x)$ (Fig. 1, point A), x_{min} is the minimum distance between punches (Fig. 1, point C), and x_{od} is the punch separation when the force returns to 0 during decompression (Fig. 1, point D).

The relation between net work and compressive work can be used to calculate the plasticity factor (PF) [33]:

$$PF = \frac{E_2}{E_2 + E_3} * 100\% \tag{7}$$

Tablet Characterization

The in-die elastic recovery was calculated by Eq. 8:

$$ER = \frac{V_r - V_m}{V_m} * 100\% \tag{8}$$

with the corrected minimal volume V_m [mm³] and the in-die recovery volume V_r [mm³]. Both were derived from the die radius and the measured thickness values during compression. The in-die recovery thickness is obtained during decompression when the upper punch force is reduced to 0.

Results and Discussion

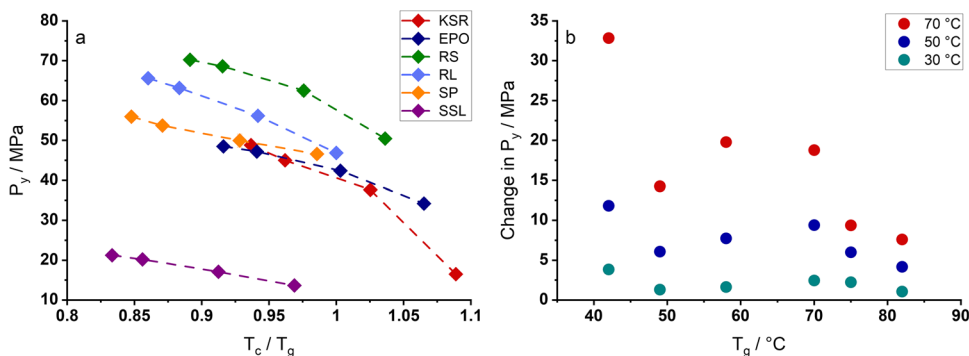
Compression Analysis

The compressibility relates the porosity reduction of a powder bed to the applied pressure [36]. For Heckel analysis, it is assumed that the volume reduction of a powder undergoing plastic deformation follows first-order kinetics [39, 40]. Typically, the plot reveals a linear region described by Eq. 4, which is enclosed by two curved sections in the low- and high-pressure regions [41]. The reciprocal value of the slope determines the yield pressure P_y for the degree of plastic deformation [42].

Previous studies included an equilibration time of 3 min per tablet for each polymer [32]. This appears reasonable to understand a material’s behavior under elevated temperatures, but fails to mimic realistic conditions during tableting if heat evolves over a prolonged time period. To serve that purpose, the tableting cycle was started immediately after filling the die. As the changes in P_y for FL were considered to be negligible in previous studies, it was excluded from the following investigation.

All polymers proved to be sensitive to elevated temperatures (Fig. 2a). The plasticity of the materials is reflected in low P_y values at ambient conditions. The closeness of the tableting temperature (T_c) to the T_g can be expressed by the homologous temperature $\frac{T_c}{T_g}$ [10, 11]. KSR with the lowest T_g shows the highest sensitivity to elevated temperatures of all polymers. P_y decreases by 33 MPa comparing a

Fig. 2 a P_y versus homologous temperature (mean ± sd, $n=3$, except KSR_{70°C}, $n=1$). **b** Change in P_y versus T_g at 250 MPa compression pressure (mean, $n=3$)



homologous temperature of 0.94 to 1.1, which corresponds to tableting temperatures of 22 and 70°C, respectively (Fig. 2b). The drastic change can be attributed to the softening of the material close to and especially above its T_g . The increased molecular mobility reduces the resistance against deformation, which affects the resulting P_y value. The decrease in P_y for EPO is surprisingly low. In previous studies with longer equilibration times, it was comparable to RS and RL. Particle size distributions revealed an x_{50} value of only $9 \pm 0.1 \mu\text{m}$ for EPO which might hinder a sufficient heat transfer due to its low bulk density if the equilibration time is short. The investigated RS and RL grades had x_{50} values of $55 \pm 0.2 \mu\text{m}$ and $58 \pm 0.7 \mu\text{m}$, respectively, which improved the flowability of the powders during filling [32].

The smallest change is observed for SP and SSL, which have the highest T_g of the investigated materials. The $\frac{T_c}{T_g}$ value is below one for all tableting temperatures. Although the temperature can locally rise drastically due to friction, the T_g will not be exceeded prior to tableting [10]. The material properties are therefore altered to a lesser extent. P_y only changes by 9 and 8 MPa, respectively.

The investigated polymers are sensitive to elevated temperatures, even if the equilibration time is kept short. Polymers with lower T_g s are more sensitive than polymers with higher T_g s [11, 26, 31].

Energy Analysis

Force–Displacement Profiles

Apart from the tableting machine and settings, the shape of force–displacement profiles is determined by material characteristics [20]. In the beginning of a tableting cycle, interparticle slippage and rearrangement reduce the volume of the powder bed at low consolidation pressures [43]. Afterwards, elastic and plastic deformation as well as fragmentation of materials lead to a significant force increase as the distance between punches decreases. The available deformation energy is impaired by energy lost through die-wall friction and particle interaction within the powder bed [4]. During decompression, the release of stored elastic energy by elastic recovery compromises the created bonding area [1, 44]. The remaining energy contains the residual stored elastic and the plastic energy (E_2 , Fig. 1). The latter can be referred to as the net work of compaction, which is used to plastically deform particles. It has been stated in literature that E_2 might be used as a surrogate for the tensile strength of tablets [21]. As plastic deformation is irreversible during decompression, the amount of stored energy within a tablet ensures a high bonding area and therefore density of the compact.

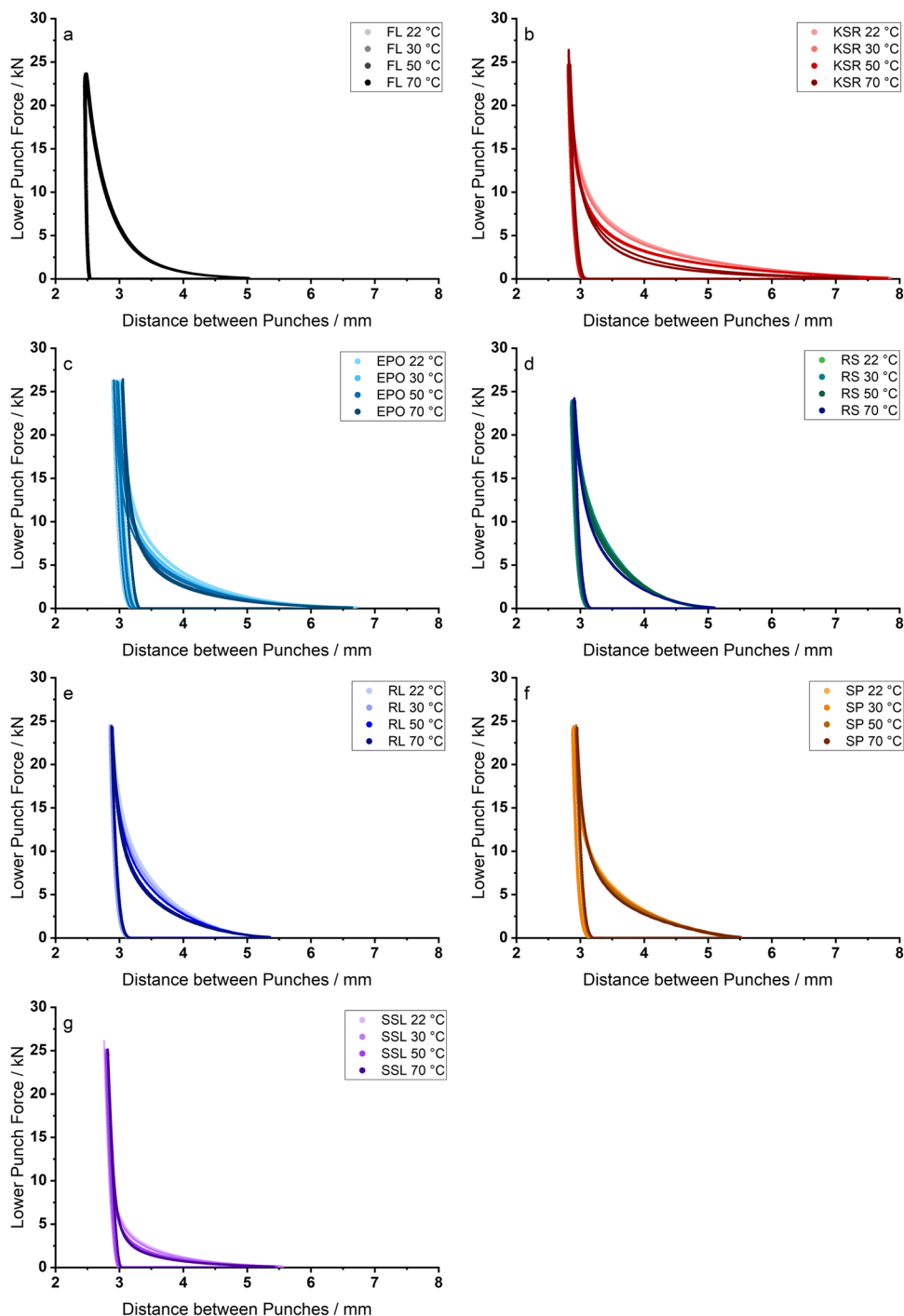
For all investigated materials except FL, the force–displacement profiles are altered when compression is performed at elevated temperatures as the physicochemical properties of materials change (Fig. 3a–g). FL served as a predominantly brittle reference with a high melting point. An increase in tableting temperature does not affect the crystal structure and therefore the compaction properties of the material (Fig. 3a). As was already observed in previous studies, the material structure is barely affected by increased temperatures, as the yield pressure does not change over the investigated temperature range [32]. Accordingly, E_2 is the same for all temperatures (Table II and Fig. 4a).

For ductile materials, the behavior is different. E_2 decreases upon temperature rise (Table II and Fig. 4a). The most prominent change can be observed for KSR and EPO with the lowest T_g s of the investigated polymers. E_2 decreases by 6.7 J from 14.6 ± 0.0 J to 7.9 ± 0.8 J and by 3.8 J from 10.5 ± 0.2 J to 6.7 ± 0.2 J, respectively. Due to the low T_g of the polymers, the physicochemical properties of the materials are altered the most. The increase in temperature allows a softening of the materials, which enhances molecular mobility and facilitates particle deformation [28].

In contrast, the net work of compaction for SSL decreases by 1.7 J from 4.4 ± 0.1 J to 2.7 ± 0.1 J only. As the T_g of SSL is higher than the maximum tableting temperature, the applied temperature affects the polymer to a lesser extent. The change in P_y was also least pronounced for SSL, which coincides with the observed findings (Fig. 2). The other polymers can be classified in between these cases. These results contradict the hypothesis that there is a direct relation between the size of the area E_2 and the tensile strength of tablets. Previous studies showed an increase in tensile strength for binary mixtures containing the same polymers at elevated temperatures [32]. It appears accurate to state that the required energy input for plastic deformation decreases when the temperature increases.

A linear fit was performed for the obtained data using the simple fit function from OriginPro to directly correlate the change in E_2 from 22 to 70°C tableting temperature to the T_g . The decrease in E_2 shows good correlation to the increase in temperature for a given polymer (Table IV). The p -values of the slopes suggest that the increase in temperature significantly affects the area E_2 . The slope for FL was not significantly different from 0. If the slope of the fit equations is plotted against the T_g of the respective materials, an exponential relationship is revealed (Fig. 4b). The lower the T_g of a polymer, the more pronounced is the decrease in E_2 . The only point deviating from the exponential curve is RL ($T_g = 70^\circ\text{C}$). If this point is excluded from the fit, the adjusted coefficient of determination (adj. R^2) changes from 0.941 (blue line) to 0.991 (black line). The slope of the regression line depending on T_g can be described by the following equation:

Fig. 3 Force–displacement profiles of **a** FL, **b** KSR, **c** EPO, **d** RS, **e** RL, **f** SP, and **g** SSL (single curves, $n = 3$)



$$\text{Slope} = -0.0370 - 18.6 * 0.879^{T_g} \left[\frac{J}{^\circ C} \right] \tag{9}$$

For RL, the slope is higher than expected considering the high T_g of the polymer, which means the temperature influence on E_2 is greater than expected (Fig. 4b, blue point). To investigate this phenomenon, the in-die elastic recovery (ER) of the polymers was evaluated.

All Eudragit grades show the highest in-die ER under ambient conditions (Fig. 4c). However, it decreases for EPO and RS upon temperature increase, while it stays the same for RL. At a tableting temperature of 70°C, RL shows the highest in-die ER of all materials (9.2%). As a result, E_2 is compromised to a larger extent, which explains the higher slope in the decrease of E_2 .

Table II Net Work of Compaction (E_2) for the Investigated Materials (mean \pm sd, $n=3$, Lower Punch)

Material	E_2/J			
	22°C	30°C	50°C	70°C
FL	9.4 \pm 0.1	9.4 \pm 0.1	9.3 \pm 0.0	9.2 \pm 0.1
KSR	14.6 \pm 0.0	13.7 \pm 0.1	11.2 \pm 0.1	7.9 \pm 0.8
EPO	10.5 \pm 0.2	9.9 \pm 0.1	8.7 \pm 0.0	6.7 \pm 0.2
RS	9.7 \pm 0.0	9.4 \pm 0.1	8.6 \pm 0.2	7.3 \pm 0.1
RL	10.1 \pm 0.0	9.7 \pm 0.0	8.7 \pm 0.0	7.3 \pm 0.2
SP	9.4 \pm 0.0	9.0 \pm 0.1	8.4 \pm 0.0	7.5 \pm 0.1
SSL	4.4 \pm 0.1	4.0 \pm 0.0	3.3 \pm 0.0	2.7 \pm 0.1

Table III Recovery Work (E_3) for the Investigated Materials (mean \pm sd, $n=3$, Lower Punch)

Material	E_3/J			
	22°C	30°C	50°C	70°C
FL	0.6 \pm 0.0	0.6 \pm 0.0	0.5 \pm 0.0	0.5 \pm 0.0
KSR	1.5 \pm 0.0	1.5 \pm 0.0	1.6 \pm 0.0	1.8 \pm 0.1
EPO	2.0 \pm 0.0	2.0 \pm 0.1	2.0 \pm 0.0	2.2 \pm 0.0
RS	1.5 \pm 0.0	1.5 \pm 0.0	1.5 \pm 0.0	1.6 \pm 0.0
RL	1.5 \pm 0.0	1.5 \pm 0.0	1.6 \pm 0.0	1.6 \pm 0.0
SP	1.5 \pm 0.0	1.5 \pm 0.1	1.6 \pm 0.0	1.6 \pm 0.0
SSL	1.8 \pm 0.1	1.8 \pm 0.0	1.8 \pm 0.0	1.8 \pm 0.0

For the ductile materials, E_3 ranges from 1.5 to 2.0 J at ambient conditions and stays similar up to 50°C tableting temperature, which coincides with previous findings (Table III) [26]. However, the in-die ER significantly increases at 70°C tableting temperature for KSR. This is also the case for E_3 , where this also applies to EPO (Fig. 4d). The observed increase for KSR and EPO at 70°C tableting temperature might be rooted in the drastic change of the elastic modulus when the T_g of a material is reached [31]. It represents the rigidity and therefore resistance against deformation of a material. When the T_g of a material is approached, it initially decreases gradually but afterwards drastically when the measuring temperature equals T_g [31]. Lower elastic moduli result in higher strain under the same stress [41]. As the densification drastically increases, the available space for

plastic flow diminishes. Further application of force results in increased elastic deformation and therefore stored elastic energy when the T_g is exceeded. The low T_g s of KSR and EPO favor the sensitivity of both materials.

For FL, the stored elastic energy is around 0.6 J for all temperatures, as it deforms mainly by brittle fragmentation, while elastic or plastic properties are negligible (Table IV).

The analysis of force–displacement plots offers valuable insights into the alteration of material behavior upon temperature rise. The sensitivity of the method proves to be sufficient to detect alterations in ductile polymers. While the T_g plays a crucial role in the changes to be expected, individual material behavior concerning aspects such as elastic recovery needs to be considered to fully characterize a material.

Fig. 4 **a** E_2 versus T (mean \pm sd, $n=3$, lower punch). **b** Exponential relationship between the change in E_2 and T_g . **c** In-die ER versus T (mean \pm sd, $n=3$). **d** E_3 versus T (mean \pm sd, $n=3$, lower punch)

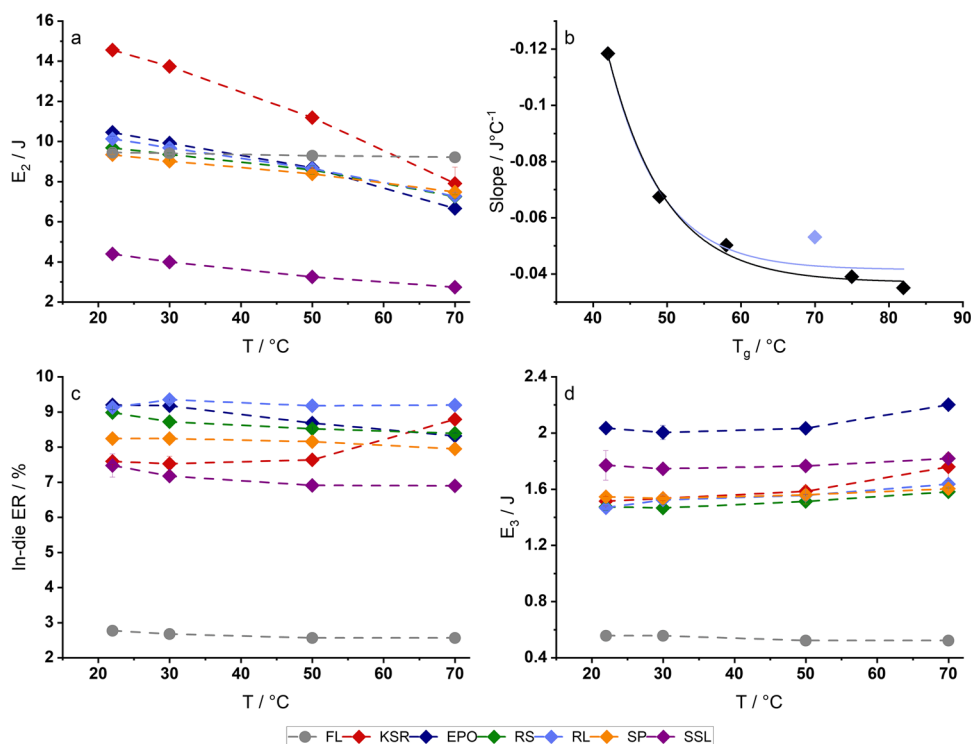


Table IV Results of the Linear Fit for E_2 Versus T

Material	Slope/ $J^{\circ}C^{-1}$	Intercept/J	p -value _{slope}	Adj. R^2
KSR	-0.119	17.2	0.00090	0.993
EPO	-0.068	12.0	0.00362	0.951
RS	-0.050	10.8	0.00161	0.994
RL	-0.053	11.3	0.00074	0.997
SP	-0.036	10.1	0.00107	1.000
SSL	-0.035	5.0	0.00227	0.979

Plasticity Factor

Plastic materials are able to create a large bonding area during compression. In contrast to brittle materials, the local stress exceeds the yield strength at an earlier stage, so that created bonds are not significantly compromised by ER [1]. A large bonding area leads to a higher solid fraction and mechanical strength. To calculate the plasticity factor (PF) as described by Stamm and Mathis [33], E_2 is divided by the sum of E_2 and E_3 (Eq. 7). The dependence of PF on the compression force and speed has been subject to several studies [20, 37, 45], as well as its dependence on the formulation [46] and particle size [47].

Several studies have interpreted the PF as the amount of plastic flow corresponding to material plasticity [20, 45–47], while other authors refer to it as the necessary energy input for plastic deformation [37]. The first interpretation seems reasonable considering the frequently postulated correlation to tablet strength [21]. When the temperature is raised, the plasticity of a material increases [1, 48]. Indeed, little recovery work during decompression leads to a high value for the plasticity of a material, which favors mechanical strength. Nevertheless, E_2 and therefore the net energy input decrease upon temperature rise, although the increase in tensile strength observed in previous studies indicates a higher plasticity [32]. As E_2 is essential for the PF calculation, it is likely PF behaves in a similar manner. All compressions

were performed with the same tableting set-up and pressure to ensure comparable values.

The highest PF is obtained for FL at all tableting temperatures (94.4–94.7%), although its plastic properties are negligible (Fig. 5a). The brittle character of the excipient leads to a high amount of fragmentation during compression. The behavior is the same for all temperatures. After the maximum compression force is reached, the punch quickly separates from the tablet during decompression due to the lack of elastic recovery. The measured force almost initially drops to 0, which lowers the size of the area E_3 (Fig. 3a). The PF value is not able to distinguish plastic deformation from brittleness, as ER can be small in both cases. In contrast to brittleness, plastic deformation is time dependent, which affects the distance between maximum compression pressure and the maximum punch displacement [20]. In order to further classify a material, both aspects need to be considered.

Ductile materials show a significant decrease in the PF when the tableting temperature is raised (p -value < 0.05) (Fig. 5a). The highest PF at ambient conditions is obtained by KSR ($90.6 \pm 0.2\%$). This means that the area E_2 is not compromised by a high ER (Fig. 4a). The other extreme is SSL, where the area E_2 is already small at ambient conditions. Therefore, the ER has a strong impact on the calculated PF. The recovery work, on the other hand, is rather pronounced (Fig. 4d). Both aspects contribute to the low value for the PF.

The assumption that increased temperatures lead to a higher plasticity of polymers is not reflected in the PF calculation. As is shown in Fig. 4a, E_2 decreases with increasing temperature, while E_3 remains constant or slightly increases (Fig. 4d). This explains the overall reduction in the PF. As the temperature is raised, the decrease in P_y generates a larger time frame for yielding and polymers become more deformable. The necessary energy input for plastic deformation decreases and a higher solid fraction is attained after compression. It appears reasonable to define the PF as the necessary energy input for plastic deformation in the context

Fig. 5 **a** PF versus T (mean \pm sd, $n=3$, lower punch). **b** Change in E_2 versus change in P_y (mean, $n=3$, lower punch)

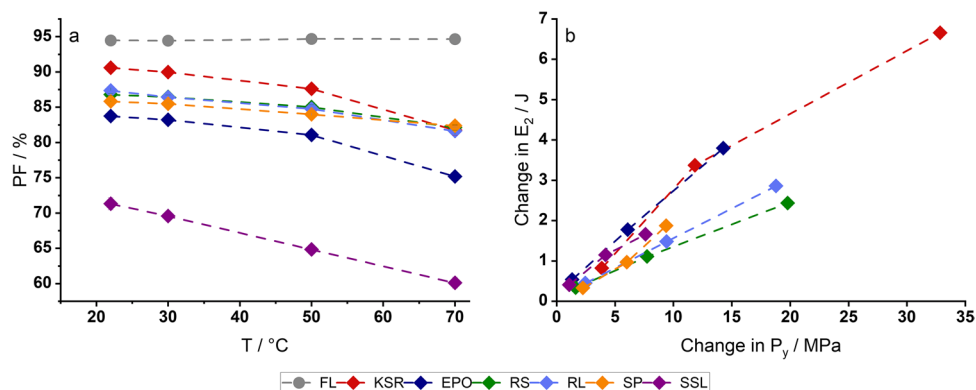


Table V Results of the Linear Fit for the Change in E_2 Versus the Change in P_y

Material	Slope/JMPa ⁻¹	Intercept/J	Adj. R^2
KSR	0.192	0.504	0.935
EPO	0.251	0.217	1.000
RS	0.115	0.174	0.997
RL	0.148	0.086	1.000
SP	0.215	-0.209	0.966
SSL	0.191	0.252	0.965

of the experimental data. However, the plasticity should increase with increasing temperature. As the plasticity values decrease with increasing temperature, the direct correlation of the PF with the plasticity of a polymer is misleading.

E_2 is strongly affected by the decrease in P_y (Fig. 5b). A relation is reasonable, as the data for in-die Heckel analysis contains parts of the force–displacement measurements to calculate the porosity of a material. FL is not depicted, as the change in P_y was not significant.

The linear fit reveals a high coefficient of determination for the change in E_2 plotted against the change in P_y when the temperature is raised (Table V). Both values decrease with increasing temperature. A reduction of P_y leads to a lower resistance against deformation and required energy input.

The calculation of PF proves to be useful to evaluate changes considering the net and recovery work of compaction. If alterations are observed in the force–displacement profile of a tableting cycle, the PF change can be assumed to directly correlate with the change in P_y as it behaves in the same manner as E_2 . However, the value should not be confused with the true plasticity of a material or its amount of plastic deformation. Although the plasticity is known to increase with increasing temperature, the PF decreases. Moreover, the highest PF value was obtained for a brittle material. Its calculation is therefore unnecessary, as the change in E_2 serves as a quick and sufficiently accurate indicator for alterations of the required energy input.

Conclusion

The energy analysis proved to be a sensitive tool for ductile polymers to detect temperature-dependent changes of the tableting behavior. Upon temperature rise, the necessary energy input for plastic deformation decreases, which is reflected in both the net work of compaction and the plasticity factor. The direct correlation of energy parameters to calculated P_y values from Heckel analysis confirms the transferability to an alteration of material properties. The alterations are especially pronounced if the T_g of the used polymers is low. Still, changes were also visible for polymers

with a $T_g >$ tableting temperature possibly due to the generation of higher temperatures in contact areas. However, the calculation of E_2 should be preferred over the calculation of the PF. It is therefore possible to identify temperature-related changes directly from the compression data, which is less time- and material-consuming than a thorough raw data analysis on an industrial scale-up.

Acknowledgements The authors would like to thank the company Medelpharm for providing the set-up for heated tableting.

Author Contribution HDG, SK, and PK: substantial contributions to the conception or design of the work; or the acquisition, analysis, or interpretation of data for the work. HDG, SK, and PK: drafting the work or revising it critically for important intellectual content. HDG, SK, and PK: final approval of the version to be published. HDG, SK, and PK: agreement to be accountable for all aspects of the work in ensuring that questions related to the accuracy or integrity of any part of the work are appropriately investigated and resolved.

Funding Open Access funding enabled and organized by Projekt DEAL. This study was funded by Medelpharm.

Data Availability Data are available upon request.

Declarations

Conflict of Interest The authors declare no competing interests.

Open Access This article is licensed under a Creative Commons Attribution 4.0 International License, which permits use, sharing, adaptation, distribution and reproduction in any medium or format, as long as you give appropriate credit to the original author(s) and the source, provide a link to the Creative Commons licence, and indicate if changes were made. The images or other third party material in this article are included in the article's Creative Commons licence, unless indicated otherwise in a credit line to the material. If material is not included in the article's Creative Commons licence and your intended use is not permitted by statutory regulation or exceeds the permitted use, you will need to obtain permission directly from the copyright holder. To view a copy of this licence, visit <http://creativecommons.org/licenses/by/4.0/>.

References

1. Sun CC. Decoding powder tableting: roles of particle adhesion and plasticity. *J Adhes Sci Technol*. 2011;25(4–5):483–99. <https://doi.org/10.1163/016942410X525678>.
2. Nyström C, Alderborn G, Duberg M, Karehill PG. Bonding surface area and bonding mechanism—two important factors for the understanding of powder comparability. *Drug Dev Ind Pharm*. 1993;19(17–18):2143–96. <https://doi.org/10.3109/03639049309047189>.
3. Ragnarsson G, Sjögren J. Work of friction and net work during compaction. *J Pharm Pharmacol*. 1983;35(4):201–4. <https://doi.org/10.1111/j.2042-7158.1983.tb02912.x>.
4. Hanus EJ, King LD. Thermodynamic effects in the compression of solids. *J Pharm Sci*. 1968;57(4):677–84. <https://doi.org/10.1002/jps.2600570431>.
5. Zavaliangos A, Galen S, Cunningham J, Winstead D. Temperature evolution during compaction of pharmaceutical powders. *J Pharm Sci*. 2008;97(8):3291–304. <https://doi.org/10.1002/jps.21229>.

6. Ketolainen J, Ilkka J, Paronen P. Temperature changes during tableting measured using infrared thermoviewer. *Int J Pharm.* 1993;92:157–66. [https://doi.org/10.1016/0378-5173\(93\)90275-K](https://doi.org/10.1016/0378-5173(93)90275-K).
7. Picker-Freyer KM, Schmidt AG. Does temperature increase induced by tableting contribute to tablet quality? *J Therm Anal Calorim.* 2004;77(2):531–9. <https://doi.org/10.1023/B:JTAN.0000038992.42788.f7>.
8. Bechard SR, Down GRB. Infrared imaging of pharmaceutical materials undergoing compaction. *Pharm Res.* 1992;9(4):521–8. <https://doi.org/10.1023/A:1015896414765>.
9. DeCrosta MT, Schwartz JB, Wigent RJ, Marshall K. Thermodynamic analysis of compact formation; compaction, unloading, and ejection. I. Design and development of a compaction calorimeter and mechanical and thermal energy determinations of powder compaction. *Int J Pharm.* 2000;198(1):113–34. [https://doi.org/10.1016/S0378-5173\(99\)00466-4](https://doi.org/10.1016/S0378-5173(99)00466-4).
10. Pilpel N, Britten JR, Onyekweli AO, Esezobo S. Compression and tableting of pharmaceutical powders at elevated temperatures. *Int J Pharm.* 1991;70(3):241–9. [https://doi.org/10.1016/0378-5173\(91\)90288-Y](https://doi.org/10.1016/0378-5173(91)90288-Y).
11. Partheniadis I, Karantzalis AE, Shah RR, Al-Zoubi N, Nikolakakis I. Influence of compression at elevated temperature on the compactibility of thermo-mechanically processed polymers. *Chem Eng Res Des.* 2020;156:64–75. <https://doi.org/10.1016/j.cherd.2020.01.035>.
12. Wurster DE, Rowlings CE, Creekmore JR. Calorimetric analysis of powder compression: I. Design and development of a compression calorimeter. *Int J Pharma.* 1995;116(2):179–89. [https://doi.org/10.1016/0378-5173\(94\)00289-H](https://doi.org/10.1016/0378-5173(94)00289-H).
13. Rowlings CE, Wurster DE, Ramsey PJ. Calorimetric analysis of powder compression: II. The relationship between energy terms measured with a compression calorimeter and tableting behavior. *Int J Pharma.* 1995;116(2):191–200. [https://doi.org/10.1016/0378-5173\(94\)00290-L](https://doi.org/10.1016/0378-5173(94)00290-L).
14. Buckner IS, Friedman RA, Wurster DE. Using compression calorimetry to characterize powder compaction behavior of pharmaceutical materials. *J Pharm Sci.* 2010;99(2):861–70. <https://doi.org/10.1002/jps.21881>.
15. DeCrosta MT, Schwartz JB, Wigent RJ, Marshall K. Thermodynamic analysis of compact formation; compaction, unloading, and ejection. II. Mechanical energy (work) and thermal energy (heat) determinations of compact unloading and ejection. *Int J Pharm.* 2001;213(1–2):45–62. [https://doi.org/10.1016/S0378-5173\(00\)00645-1](https://doi.org/10.1016/S0378-5173(00)00645-1).
16. Klinzing GR, Zavaliangos A, Cunningham J, Mascaro T, Winstead D. Temperature and density evolution during compaction of a capsule shaped tablet. *Comput Chem Eng.* 2010;34(7):1082–91. <https://doi.org/10.1016/j.compchemeng.2010.04.012>.
17. Gharaibeh SF, Aburub A. Use of first derivative of displacement vs. force profiles to determine deformation behavior of compressed powders. *AAPS PharmSciTech.* 2013;14(1):398–401. <https://doi.org/10.1208/s12249-013-9928-2>.
18. de Blaey CJ, Polderman J. Compression of pharmaceuticals. I. The quantitative interpretation of force-displacement curves. *Pharmaceutisch Weekblad.* 1970;105(9):241–50.
19. Higuchi T, Arnold R, Tucker S, Bussé L. The physics of tablet compression. I. A preliminary report†. *J Am Pharma Assoc Am Pharma Assoc.* 2006;41:93–6. <https://doi.org/10.1002/jps.3030410214>
20. Antikainen O, Yliruusi J. Determining the compression behaviour of pharmaceutical powders from the force–distance compression profile. *Int J Pharm.* 2003;252(1):253–61. [https://doi.org/10.1016/S0378-5173\(02\)00665-8](https://doi.org/10.1016/S0378-5173(02)00665-8).
21. Ritschel WA, Bauer-Brandl A. *Die Tablette: Handbuch der Entwicklung, Herstellung und Qualitätssicherung: ECV - Editio Cantor Verlag; 2012.*
22. Kawakita K, Lüdde K-H. Some considerations on powder compression equations. *Powder Technol.* 1971;4(2):61–8. [https://doi.org/10.1016/0032-5910\(71\)80001-3](https://doi.org/10.1016/0032-5910(71)80001-3).
23. Ilkka J, Paronen P. Prediction of the compression behaviour of powder mixtures by the Heckel equation. *Int J Pharm.* 1993;94(1):181–7. [https://doi.org/10.1016/0378-5173\(93\)90022-8](https://doi.org/10.1016/0378-5173(93)90022-8).
24. Picker KM, Hoag SW. Characterization of the thermal properties of microcrystalline cellulose by modulated temperature differential scanning calorimetry. *J Pharm Sci.* 2002;91(2):342–9. <https://doi.org/10.1002/jps.10018>.
25. Botha SA, Lötter AP. Compatibility study between oxprenolol hydrochloride, temazepam and tablet excipients using differential scanning calorimetry. *Drug Dev Ind Pharm.* 1990;16(2):331–45. <https://doi.org/10.3109/03639049009114889>.
26. Cespi M, Bonacucina G, Casettari L, Ronchi S, Palmieri GF. Effect of temperature increase during the tableting of pharmaceutical materials. *Int J Pharm.* 2013;448(1):320–6. <https://doi.org/10.1016/j.ijpharm.2013.03.014>.
27. Casettari L, Bonacucina G, Cespi M, Perinelli DR, Micheli M, Cacciatore I, et al. Effect of manufacturing temperature and molecular weights on compression, mechanical and dissolution properties of PEO matrix tablets. *Journal of Drug Delivery Science and Technology.* 2016;32:236–40. <https://doi.org/10.1016/j.jddst.2015.05.005>.
28. Cowie JMG, Arrighi V. *Polymers: chemistry and physics of modern materials.* Boca Raton: CRC Press; 2007.
29. USPC. Chapter <1062> tablet compression characterization. USP 41-NF 36. Rockville, MD: USPC; 2018. p. 7042–53.
30. Van Der Voort MK, Vromans H, Bolhuis G, Lerk C. Influence of plasticizers on tableting properties of polymers. *Drug Dev Ind Pharm.* 1998;24(3):261–8. <https://doi.org/10.3109/03639049809085618>.
31. Van der Voort MK, Zuurman K, Van Steenberghe MJ, Hennink WE, Vromans H, Bolhuis GK, et al. Effect of compaction temperature on consolidation of amorphous copolymers with different glass transition temperatures. *Pharm Res.* 1997;14(4):415–9. <https://doi.org/10.1023/A:1012078928297>.
32. Grumann HD, Klinken S, Kleinebudde P. Influence of temperature on the compression behavior of pharmaceutical excipients. *Int J Pharma.* 2022;628:122305. <https://doi.org/10.1016/j.ijpharm.2022.122305>.
33. Stamm A, Mathis C. Verpressbarkeit von festen Hilfsstoffen für Direkttablettierung. *Acta Pharm Technol.* 1976;22(SUPPL. 1):7–16.
34. Luebbert C, Stoyanov E, Sadowski G. Phase behavior of ASDs based on hydroxypropyl cellulose. *Int J Pharma X.* 2021;3:100070. <https://doi.org/10.1016/j.ijpx.2020.100070>.
35. Merck: Safety Data Sheet PARTECK LUB MST. www.pharm.aexcipients.com/product/parteck-lub-mst-magnesium-stearate-vegetable-grade/?attachment_id=148476&download_file=f6xjm1xqzdyna (2017). Accessed 08/12/2022.
36. USPC. Chapter <699> density of solids. USP 41-NF 36. Rockville, MD: USPC; 2018. p. 6453–5.
37. Krok A, Mirtic A, Reynolds GK, Schiano S, Roberts R, Wu CY. An experimental investigation of temperature rise during compaction of pharmaceutical powders. *Int J Pharm.* 2016;513(1–2):97–108. <https://doi.org/10.1016/j.ijpharm.2016.09.012>.
38. Hauschild K, Picker-Freyer KM. Evaluation of tableting and tablet properties of Kollidon SR: the influence of moisture and mixtures with theophylline monohydrate. *Pharm Dev Technol.* 2006;11(1):125–40. <https://doi.org/10.1080/108374505000464289>.
39. Heckel R. Density-pressure relationship in powder compaction. *Trans Met Soc, AIME.* 1961;221:671–5.
40. Heckel R. An analysis of powder compaction phenomena. *Trans Metall Soc AIME.* 1961;221:1001–8.

41. Sun C, Grant D. Influence of elastic deformation of particles on Heckel analysis. *Pharm Dev Technol.* 2001;6:193–200. <https://doi.org/10.1081/PDT-100000738>.
42. Duberg M, Nyström C. Studies on direct compression of tablets XVII. Porosity—pressure curves for the characterization of volume reduction mechanisms in powder compression. *Powder Technol.* 1986;46(1):67–75. [https://doi.org/10.1016/0032-5910\(86\)80100-0](https://doi.org/10.1016/0032-5910(86)80100-0).
43. Wray PE. The physics of tablet compaction revisited. *Drug Dev Ind Pharm.* 1992;18(6–7):627–58. <https://doi.org/10.3109/03639049209058556>.
44. Jivraj M, Martini LG, Thomson CM. An overview of the different excipients useful for the direct compression of tablets. *Pharm Sci Technol Today.* 2000;3(2):58–63. [https://doi.org/10.1016/S1461-5347\(99\)00237-0](https://doi.org/10.1016/S1461-5347(99)00237-0).
45. Ren G, Clancy C, Tamer TM, Schaller B, Walker GM, Collins MN. Cinnamyl O-amine functionalized chitosan as a new excipient in direct compressed tablets with improved drug delivery. *Int J Biol Macromol.* 2019;141:936–46. <https://doi.org/10.1016/j.ijbio mac.2019.08.265>.
46. Kása P, Bajdik J, Zsigmond Z, Pintye-Hódi K. Study of the compaction behaviour and compressibility of binary mixtures of some pharmaceutical excipients during direct compression. *Chem Eng Process.* 2009;48(4):859–63. <https://doi.org/10.1016/j.cep.2008.11.002>.
47. Kelemen A, Szalay A, Sovány T, Pintye-Hódi K. Role of the particle size of sorbitol during the compression of common tablets and prediction of mini-tablet compression parameters. *Chem Eng Res Des.* 2015;104:814–8. <https://doi.org/10.1016/j.cherd.2015.10.028>.
48. Osei-Yeboah F, Chang S-Y, Sun CC. A critical examination of the phenomenon of bonding area - bonding strength interplay in powder tableting. *Pharm Res.* 2016;33(5):1126–32. <https://doi.org/10.1007/s11095-016-1858-8>.

Publisher's Note Springer Nature remains neutral with regard to jurisdictional claims in published maps and institutional affiliations.